PHYSICAL REVIEW A **73**, 020707(R) (2006)

Experimental and theoretical studies of the photoionization cross section of Fe^{4+}

J. M. Bizau,[1] C. Blancard,[2] D. Cubaynes,[1] F. Folkmann,[3] D. Kilbane,[4] G. Faussurier,[2] H. Luna,[4] J. L. Lemaire,[2] J. Blieck,[1] and F. J. Wuilleumier[1]

[1]*Laboratoire d'Interaction des Rayons X avec la Matière (LIXAM), UMR 8624 du CNRS, Université Paris-Sud, Bâtiment 350, 91405 Orsay Cedex, France*

[2]*CEA DAM Ile-de-France, DPTA, Boîte Postale 12, F-91680 Bruyères-le-Châtel Cedex, France*

[3]*Department of Physics and Astronomy, University of Aarhus, DK-8000 Aarhus C, Denmark*

[4]*National Centre for Plasma Science and Technology, School of Physical Sciences, Dublin City University, Glasnevin, Dublin 9, Ireland*

(Received 20 December 2005; published 24 February 2006)

We have measured the absolute photoionization cross section of the Fe^{4+} ion between 59 and 140 eV photon energy, including the region of the $3p \rightarrow 3d$ excitations. To interpret the data we have performed calculations using a code developed for the determination of the spectral opacity of hot plasmas. We have also compared our measurements with the results of several *R*-matrix calculations. In short, both theoretical approaches describe qualitatively the results of the experiment in the $3p$-$3d$ excitation region.

DOI: 10.1103/PhysRevA.73.020707 PACS number(s): 32.80.Fb, 32.80.Hd

Iron (Fe) is the heaviest element with a significant cosmic abundance. Thus spectral features of Fe ions are observed in many astrophysical plasmas [1,2]. Fe ions are therefore of great diagnostic value across most photon energy ranges, from the far infrared to hard x-rays. Very often, photoionization processes, together with recombination, drive the ionization states of the elements in plasmas, explaining why the values of the cross sections for these processes are required for modeling the plasmas and the calculation of their opacity. The astrophysical need for atomic data has mainly motivated a large number of extensive theoretical developments. Direct photoionization cross sections have been first calculated for the ions of the most abundant elements using one-electron models [3–5], thus neglecting most of the electron correlation effects and ignoring the resonant processes. Later, the *R*-matrix method in the close coupling (CC) approximation was used by several international collaborations [Opacity Project (OP), Iron Project, RmaX Network] to produce large data sets of atomic data [6–8].

Together with the transition elements, the low-charged states of Fe ions occupy a special position regarding fundamental atomic physics. The large number of allowed terms arising from the open $3d$ subshell results in very complex atomic systems that are extremely difficult to describe due to the strong influence of electron correlations in the initial state. The situation is further complicated in the region of the so-called $3p \rightarrow 3d$ giant resonance by the addition of one hole in the $3p$-inner subshell, producing numerous overlapping resonance lines with large natural widths [9]. Considering the complexity of the theoretical description of these systems, experimental benchmarks are required for testing and improving the theoretical methods. The theoretical complexity is matched by the experimental difficulties in producing beams of Fe ions, arising from the high temperature required for the evaporation of metallic iron. In addition, the existence of many metastable states in the ionic beam further complicates the interpretation of the observed spectra. For these reasons, most available experimental data up to now have been obtained on neutral Fe [9]. For the Fe ions, photoionization cross sections have been measured for Fe^{+} only [10], revealing that some discrepancies do exist between the experimental and available theoretical values.

Focusing now on the Fe^{4+} ion, several theoretical investigations have been performed to determine energy levels, oscillator strengths for excitations, and ionization cross sections. As part of OP, photoionization cross sections for this ion in the ground state and in many excited states have been calculated using the *R*-matrix method [11], neglecting however inner-shell excitations and relativistic effects. Later, the $3p$ excitations were included as well as the relativistic effects using the Breit-Pauli approximation [12], to obtain also, in a self-consistent way, the partial photoionization cross sections and recombination rates [2]. In the frame of the RmaX network, inner-shell photoionization was calculated over a wide energy range for this ion in the ground state [13]. Energy levels and oscillator strengths for the $3d$ excitations were also computed using the *R*-matrix [14] and multiconfiguration Dirac-Fock (MCDF) methods [15].

We present in this paper the results of our measurements and calculations of the photoionization cross section for Fe^{4+} between 59 and 140 eV, including the region of the $3p \rightarrow 3d$ excitations. The choice of the Fe^{4+} ion was mainly guided by two considerations: the difficulty to describe Fe ions generally increases for the very low charged states due to the enhancement of electron correlation effects; Fe^{4+} is the most highly charged ion of the isonuclear series for which $3p \rightarrow 3d$ excitations are above the first ionization threshold, allowing us to observe them in the ionization spectra. Among the various *R*-matrix calculations, however, one of them predicts the existence of broad and strong $3p \rightarrow 3d$ resonances above the threshold for the ion in the ground state [12], while the other two do not [11,13].

Our measurements were performed at the ASTRID storage ring facility of the Aarhus University, with the same setup as previously used for the experiment on the Fe^{+} ion [10], with one major difference, however: an electron cyclotron resonance ion source (ECRIS) was used for the production of the Fe^{4+} beams [16]. In short, Fe ions are produced

within the ECRIS with the help of a resistively heated microoven [17] introduced into the plasma chamber. Temperatures of about 1300 °C were needed to obtain a vapor pressure of about 10^{-3} mbar in the chamber. After extraction by a 2 kV voltage and selection of Fe^{4+} with a dipole magnet, the photoionization cross section was obtained by merging the 8 keV Fe^{4+} ion beam with a monochromatized photon beam emitted from the ASTRID undulator, and measuring the resulting Fe^{5+} ion yield. In addition, we determined all parameters needed to extract the measured cross section, including the spatial overlap between the photon and ion beams [16]. In our study, the spectral resolution was around 0.3% over the 60–80 eV photon energy range, and about 1% in the higher energy region which is free of strong resonances. In the present case, we took into account the presence of N^+ ions in the Fe^{4+} target beam, while neglecting a possible small contamination by N_2^{2+} ions. The relative population of N^+ ion was determined by measuring the N^{2+} ion yield in the 40–45 eV photon energy range and comparing the resulting cross section with the previously measured value [18]. This procedure was repeated after each Fe^{4+} measurement, keeping unchanged the experimental conditions in the production and the transport of the target ion beam up to the interaction region. An Al filter was used to suppress the contribution due to higher order radiation diffracted by the monochromator. One should note that, even though the percentage of N^+ ions in the $1s^22s^22p^2\ ^3P$ ground term and ^1D, ^1S metastable terms is different in our experiment when compared to the previous work on Fe^+ ions, this difference does not affect the results since the value of the N^+ direct photoionization cross section between 40 and 45 eV photon energy is almost independent of the initial terms [19]. Typical ion beam currents in the interaction region were close to 15 nA, including a 30% contribution of N^+ ions. As a consequence of this procedure, our total uncertainty, which is usually 10% to 15% in our cross section measurements [16], was here between 15% and 20%.

The near-threshold photoionization cross section, resulting from six averaged independent measurements, is presented in the upper panel of Fig. 1. The vertical bars above the spectrum give the energy position of the thresholds for the ground and metastable levels of the $3p^63d^4$ configuration [20]. The threshold for the Fe^{4+} ion in the $3p^63d^4\ ^5D_0$ ground level is at 75.010 eV. An edge is actually visible at 75 eV, but an intense signal is also observed down to 60 eV, which is the energy threshold for the highest metastable level, demonstrating that the ions produced in the ECRIS in all levels of the $3p^63d^4$ configuration are contributing to the signal. In addition to the edges associated with these thresholds, broad resonant structures are clearly observed. Some similarities with the spectra of neutral Fe [21] and the Fe^+ ion [10] are remarkable with the existence of two broad and asymmetric structures. Nevertheless, in the case of the Fe^{4+} ion, they are shifted by 19 eV towards higher photon energy and their intensity is strongly reduced.

We have performed our calculations using a spectral opacity code. The self-consistent average atom for laboratory plasmas (SCAALP) code with detailed line accounting [22] has been modified to calculate the total photoionization cross section from the $3p^63d^4$ configuration of Fe^{4+}, including 34 levels, as a sum of direct and resonant contributions between

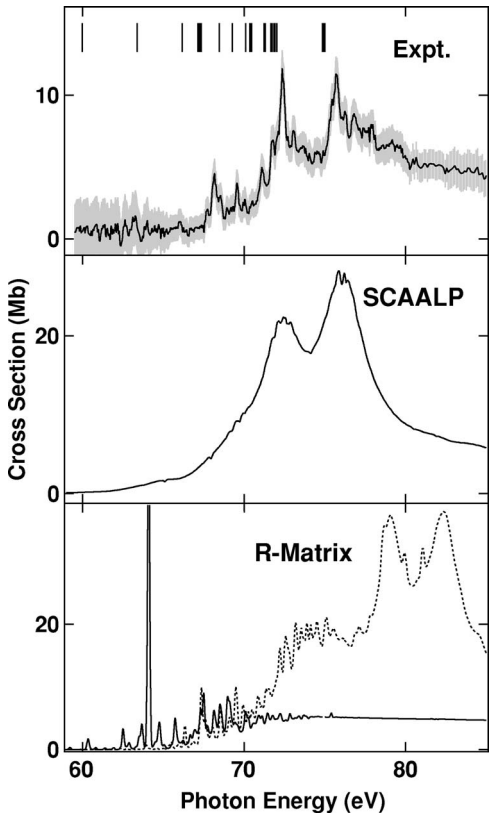

FIG. 1. Variation of the photoionization cross sections of the Fe^{4+} ion as a function of the photon energy. Upper panel: present experimental results. The zone in gray represents the statistical uncertainty. The ionization thresholds for the Fe^{4+} ions in the ground and metastable levels are shown as the vertical bars on the upper panel (Ref. [20]). Middle panel: synthetic spectrum reconstructed from the calculated SCAALP photoionization cross sections. Lower panel: synthetic spectra reconstructed from the *R*-matrix calculations available in the TOPbase (Ref. [11]) (solid line) and in Refs. [2,12] (dotted line).

pairs of configurations. Bound-bound and bound-free oscillator strengths were calculated in the length form of the electric dipole operator. The excited configurations $3p^53d^5$, $3p^53d^44s$, and $3p^53d^44d$ have been considered. The direct photoionization cross section to $3p^63d^3$ and $3p^53d^4$ configurations were evaluated from one-electron calculations. The energy thresholds were estimated from configuration average energies. The edges were convolved by a Gaussian profile with a variance equal to the sum of the initial and final configuration energy variances. The resonant photoionization cross sections were calculated performing detailed line accounting in pure jj coupling. Only photoexcited levels above the first ionization limit were retained, and a statistical population of the initial levels was assumed. A Lorentzian profile was used for each line shape with a full width at half maximum (FWMH) equal to the natural width. Using one-electron calculations, we found that natural widths are dominated by autoionization rates and are equal to 2.30 eV, 1.61 eV, and 0.61 eV for $3p^53d^5$, $3p^53d^44s$, and $3p^53d^44d$, respectively. The resulting spectrum was then convolved with a square function 150 meV width to account for the finite spectral resolution. The result is shown in the middle

panel of Fig. 1. It reproduces satisfactorily the experimental spectrum, in particular the direct photoionization cross section in the high energy part of the spectrum and the energy of the two dominant resonant structures. It shows that, as in the case of neutral Fe and the Fe^+ ion, most of the observed structures are due to $3p \rightarrow 3d$ excitations. Quantitatively, however, the intensity of the lines is overestimated by the calculations.

A better model of the experimental spectrum would require the introduction of configuration interaction effects. In particular, it has been shown that $3p^2 \rightarrow 3d^2$ excitations strongly influence both the energy and intensity of the $3p^6 3d^N \rightarrow 3p^5 3d^{(N+1)}$ transitions in the Fe group elements [23]. Quantum interferences between the direct and resonant channels contribute also to modify the intensity of the resonances, resulting in the Fano profile of these lines. These effects are taken into account in the *R*-matrix calculations. The synthetic spectrum resulting from the OP study with 15 *LS* terms CC expansion [11] is shown in the lower panel of Fig. 1, together with the one from a relativistic *R*-matrix calculations using 34 terms CC expansion [2,12]. The summation of the individual photoionization cross sections was weighted by the statistical weight of the $3p^6 3d^4\ ^{2S+1}L$ terms, and the results were convolved with a Gaussian function with a 150 meV FWMH to describe the experimental broadening. The contribution from the ^1I term, not available in the TOP base, is missing in the OP spectrum. The OP synthetic spectrum reproduces very well the direct photoionization spectrum above 80 eV, but fails to describe the resonant structures, as expected from the fact that it does not include inner-shell excitations and relativistic effects. Also, it predicts the existence of an intense resonance near 64.1 eV arising from the second of the ^3P terms, which is not observed in the experimental spectrum. In opposite, the other *R*-matrix calculations, including the $3p \rightarrow 3d$ excitations, reproduce qualitatively the two dominant resonant structures, but somewhat overestimate their energy position and absolute cross section values.

Our SCAALP calculations reveal that the whole resonant structure is produced from ions in the metastable states (less than 1% would result from the contribution of the ground level), in disagreement with the 34 terms *R*-matrix calculations [2,12] which predict the existence of two broad resonances around 78.6 and 78.9 eV in the photoionization cross section of the ion in the ground level, likely to be associated with $3p \rightarrow 3d$ excitations. These structures are not present in more recent *R*-matrix results, obtained using a lower CC expansion [13]. Although the high number of metastable levels makes our measurements not able to definitely test the validity of these various predictions, this test can be performed on the direct photoionization process. Since the intensity of these processes is almost independent of the initial level of the ion within the same configuration, the cross section we measured outside of the resonant region is then a good representation of the direct photoionization cross section for these ions in the ground level. Our results up to 140 eV photon energy are shown in Fig. 2 as the continuous curve. Some weak structures are observed near 100 and 120 eV. These energies are close to the calculated values for the opening of the $3p^6 3d^2 4s\varepsilon l$ [12] and $3p^5 3d^3 \varepsilon l$ [13] ionization channels, respectively. The results of the one-electron calculations [3–5] are also reproduced in Fig. 2. All produce values of the direct photoionization cross section in good agreement with experiment, well within the uncertainty. The results of the OP *R*-matrix calculations [11] are also in good agreement with experiment in the 80–140 eV energy range, while the two more recent *R*-matrix calculations [12,13] predict cross section values higher by a factor of about 2.

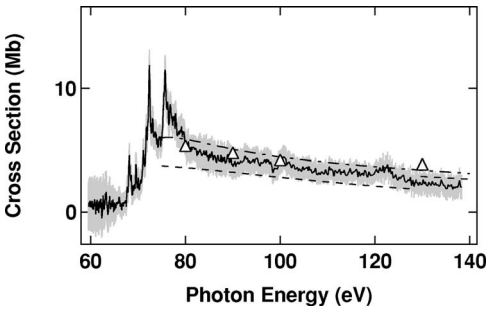

FIG. 2. Variation of the photoionization cross sections of the Fe^{4+} ion over the whole photon energy range. The present experimental results (solid line) are compared with the results by Reilman and Manson [open triangles, (Ref. [3])] and by Verner *et al.* (dashed line Ref. [4], and dash-dotted line Ref. [5]).

We have summarized in Table I the values of the oscillator strengths *f* for the $3p \rightarrow nl$ resonant and $3d, 3p \rightarrow \varepsilon l$ direct transitions measured and calculated in our work, together with the results of other theoretical calculations [4,5,11,12]. They were obtained by the integration of the respective spectra shown in Fig. 1 between 60 and 140 eV. The partition of the experimental values into discrete and continuum transitions was estimated by an adjustment of the continuous part of the experimental spectrum to an analytical form given by one-electron calculations [5]. As compared to the Fe^+ ion, our measured total oscillator strength is smaller by a factor of 2 ($f = 5.4 \pm 0.8$ for Fe^+) [10]. The decrease in the screening of the nucleus attraction resulting from the removal of outer electrons moves the ionization threshold towards higher energies, thus reducing the integrated strength in the direct photoionization process. Part of the $3p \rightarrow 3d$ transitions are also shifted below this threshold and do not contribute any more to autoionization (about half of their oscillator strength

TABLE I. Integrated oscillator strengths *f*.

	Expt.	SCAALP	Ref. [11]	Refs. [2,12]	Ref. [4]	Ref. [5]
$3p \rightarrow nl$	≈0.6	1.8				
$3d, 3p \rightarrow \varepsilon l$	≈1.9	2.2			1.6	2.6
Total	2.5±0.5	4.0	2.6	6.7		

according to our SCAALP calculations). The OP *R*-matrix calculations [11] reproduce correctly the total intensity of the cross section, while the calculations performed with a larger CC expansion [12] predict a significantly higher intensity. Our calculated $3p \rightarrow 3d$ excitation SCAALP oscillator strength is also overestimated, showing that the introduction of natural broadening is not sufficient to bring the intensity of the lines in complete agreement with the experimental values. Several reasons can explain this discrepancy: some of the $3p^5 3d^5$ excited levels may decay by fluorescence and are not observed in our measurements; the calculated thresholds are lower than the experimental values so that the calculations included excited states that also decay only via fluorescence; configuration mixing and interference effects are not included in the calculations.

In conclusion, our measured absolute values of the direct photoionization cross section for the Fe^{4+} ion between 59 and 140 eV are in good agreement with the results of our SCAALP calculations, as well as the one-electron and OP *R*-matrix calculations. More recent *R*-matrix results significantly overestimate this cross section. In contrast, all calculations fail to reproduce quantitatively the $3p \rightarrow 3d$ excitations region.

The authors would like to acknowledge the support of the European Community Research Infrastructure Action under FP6 Structuring the European Reseach programme (IA-SFS, Contract No. RII3-CT-2004-506008) and to thank M. A. Bautista for communication of his detailed results. They are also grateful to the ISA staffs of the Aarhus University for their helpful assistance.

[1] S. R. Becker and K. Butler, Astron. Astrophys. **265**, 647 (1992).
[2] S. N. Nahar and M. A. Bautista, Astrophys. J., Suppl. Ser. **120**, 327 (1999) and references therein.
[3] R. F. Reilman and S. T. Manson, Astrophys. J., Suppl. Ser. **40**, 815 (1979).
[4] D. A. Verner *et al.*, At. Data Nucl. Data Tables **55**, 233 (1993).
[5] D. A. Verner and D. G. Yakovlev, Astron. Astrophys., Suppl. Ser. **109**, 125 (1995).
[6] The Opacity Project Team, *The Opacity Project* (Institute of Physics, Bristol, 1995), Vols. 1 and 2.
[7] D. G. Hummer *et al.*, Astron. Astrophys. **279**, 298 (1993).
[8] K. A. Berrington, in *Proceedings of Atomic Data Needs for X-ray Astronomy, 2000*, edited by M. A. Bautista, T. R. Kallman, and A. K. Pradhan (NASA, Washington, DC, 2000), p. 65.
[9] B. Sonntag and P. Zimmermann, Rep. Prog. Phys. **55**, 911 (1992).
[10] H. Kjeldsen *et al.*, J. Phys. B **35**, 3655 (2002).
[11] K. Butler (unpublished). The data are available from TOPBase via World Wide Web at http://vizier.u-strasbg.fr/topbase/topbase.html
[12] M. A. Bautista, Astron. Astrophys., Suppl. Ser. **119**, 105 (1996).
[13] K. A. Berrington and C. Ballance, J. Phys. B **34**, 2697 (2001).
[14] S. N. Nahar *et al.*, Astron. Astrophys., Suppl. Ser. **144**, 141 (2000).
[15] S. M. O'Malley, D. R. Beck, and D. P. Oros, Phys. Rev. A **63**, 032501 (2001).
[16] H. Kjeldsen *et al.*, Nucl. Instrum. Methods Phys. Res. B **234**, 349 (2005).
[17] R. Lang *et al.*, Rev. Sci. Instrum. **71**, 651 (2000).
[18] H. Kjeldsen *et al.*, Astrophys. J., Suppl. Ser. **138**, 219 (2002).
[19] D. Luo and A. K. Pradan, J. Phys. B **22**, 3377 (1989); data are available in the TOPbase.
[20] J. Sugar and C. Corliss, J. Phys. Chem. Ref. Data **14**, 407 (1985) and references therein.
[21] H. Feist *et al.*, Phys. Rev. A **53**, 760 (1996).
[22] P. Renaudin *et al.*, J. Quant. Spectrosc. Radiat. Transf. **99**, 511 (2006).
[23] P. Quinet and J. E. Hansen, J. Phys. B **28**, L213 (1995).